*Vietnam Journal of Science and Technology* ***63*** *(5) (2025) 875-885*

doi:10.15625/2525-2518/18333

# Synthesis and characterization of the blends of deproteinized natural rubber-graft-polystyrene and regenerated cellulose

**Tran Thi Tuyet, Vu Trung Nam, Nguyen Quynh Vi, Nguyen Thu Ha, Tran Thi Thuy*, Nguyen Ngoc Mai***

*Hanoi University of Science and Technology, No. 1 Dai Co Viet street, 10000 Ha Noi, Viet Nam*

*Emails: thuy.tranthi3@hust.edu.vn, mai.nguyenngoc@hust.edu.vn

Received: 4 November 2024; Accepted for publication: 29 August 2025

**Abstract.** Cellulose and natural rubber (NR) are two widely commercialized natural polymers. The combination of them in a composite material has the potential to further expand their application capabilities. In this study, the preparation and characterization of composites formed by deproteinized natural rubber graft copolymerization with styrene (DPNR-graft-PS) and regenerated cellulose (RC) were investigated. In which DPNR-graft-PS was employed as the matrix. The RC was employed as a reinforcing phase or discontinuous phase. The combination of these two polymers was made by coprecipitating from a mixture of modified natural rubber and RC with different RC/DPNR-graft-PS ratios. The characterization of the new biocomposite materials was investigated by Fourier transform infrared spectroscopy (FTIR) and X-ray diffraction (XRD). The morphology was analyzed by scanning electron microscopy (SEM). The enhancement in thermal properties was examined through thermogravimetric analysis (TGA) and differential scanning calorimetry (DSC). The findings obtained showed that the novel structure of RC/DPNR-graft-PS exhibited excellent properties.

*Keywords:* natural rubber, styrene, regenerated cellulose, morphology, thermal properties.

*Classification numbers*: 1.3.3, 2.9.3, 2.9.4.

## 1. INTRODUCTION

Natural rubber (NR) is a natural polymer, known for many outstanding mechanical properties such as excellent elasticity, high strength, and good abrasion resistance [1, 2]. NR is widely used in various applications [3, 4]. However, the usage conditions of NR are limited due to its physical, chemical and especially thermal properties. Previous research has shown that vulcanization with a curing system can enhance NR's heat aging resistance [5 - 7]. Nevertheless, the disadvantage of sulfur is its toxicity to people's health and the environment [8]. A recommended alternative is cellulose, the most abundant natural polymer, which is renewable, biodegradable, and non-toxic [9 - 11]. Using cellulose protects human health and the environment while also improving the thermal properties of NR.

Regenerated cellulose (RC) was used as a reinforcing agent in our work. The RC is usually formed by dissolving cellulose, however the solubility of cellulose in common solvents is difficult [12]. There are some special solvents that can dissolve cellulose such as Cu-ethylenediamine, Cadmium-ethylenediamine, and N-methylmorphine N-oxide. However, these solvents are harmful to the environment and human health. Therefore, studies on solvent systems that can dissolve cellulose and are environmentally friendly are being developed [13]. The solvent system consisting of alkaline/additive/water was chosen so that cellulose could be easily and effectively dispersed in the modified NR [14 - 17].

The combination of RC and NR meets expected properties and protects people's health and the environment[11]. However, the heat resistance of RC-reinforced NR is lower than that of sulfur-vulcanized NR, specifically 360 $^{o}$C [18] compared to 380 $^{o}$C [19]. Polystyrene (PS) copolymerized from styrene monomer is known to have high heat resistance besides polyvinyl alcohol (PVA) [20], polycaprolactone (PCL) [21], polylactic acid (PLA) [22, 23], and poly(butylene succinate) (PBS) [24, 25]. For this reason, the graft copolymerization of deproteinized natural rubber (DPNR) with styrene (DPNR-graft-PS) using RC as a reinforcement was studied to obtain a novel biocomposite material with similar or even higher heat resistance compared to the use of sulfur for vulcanizing NR. A report on the use of RC reinforcement for modified rubber is not currently available.

This study focuses on the preparation and characterization of RC/DPNR-graft-PS. We first dissolved cellulose in an NaOH/urea aqueous solution. The resulting cellulose solution was then co-precipitated with DPNR-graft-PS using ethanol to form the new RC/DPNR-graft-PS material. Excess polymers were removed via Soxhlet extraction to ensure purity. The final material's structure, morphology, and thermal properties were then characterized using Fourier transform infrared spectroscopy (FT-IR), X-Ray diffraction (XRD), scanning electron microscope (SEM), thermogravimetric analysis (TGA) and differential scanning calorimetry (DSC).

## 2. MATERIALS AND METHODS

### 2.1. Materials

Highly ammoniated natural rubber (HANR) with a dried rubber content of about 60 wt.% was provided by Merufa Company (Ho Chi Minh City, Viet Nam). Sodium dodecyl sulfate (SDS, > 97.0 %) and styrene (ST, > 99 %) were obtained from Tokyo Chemical Industry Co. (Tokyo, Japan). Urea (≥ 99 %) was supplied by Nacalai Tesque, Inc (Kyoto, Japan). Sodium hydroxide (NaOH, reagent grade, ≥ 98 %, pellets), ethanol (ACS reagent) and microcrystalline cellulose (MCC, 20 µm, powder) were purchased from Sigma-Aldrich.

### 2.2. Methods

*2.2.1. Preparation of DPNR-graft-PS by graft-copolymerization between styrene and DPNR*

The DPNR-graft-PS fabrication process involves three steps. First, natural rubber (NR) is deproteinized with urea and SDS to prevent side reactions. Next, the DPNR-graft-PS is synthesized through graft-copolymerization of the deproteinized rubber (DPNR) and styrene, using a TBHPO/TEPA redox initiator system. Finally, unreacted styrene monomers are removed via a vacuum rotary evaporator to purify the final product. These procedures were presented in our previous studies [26, 27].

*2.2.2. Preparation of a homogenous cellulose solution*

To dissolve microcrystalline cellulose (MCC), a homogenous mixture of 20 µm MCC, sodium hydroxide, urea, and water (in a 7/12/81 mass ratio) was stirred for an hour. The mixture was then frozen at -12 °C for 24 hours. After defrosting at room temperature, it became a transparent 4 wt.% MCC solution.

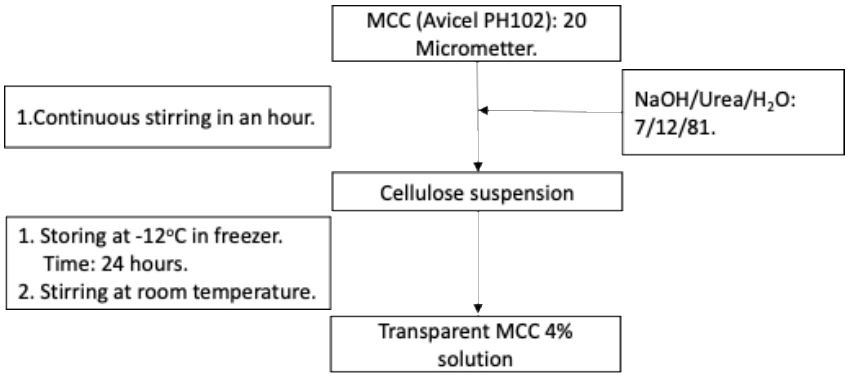


*Figure 1.* Scheme for the preparation of a homogenous cellulose solution.

*2.2.3. Reinforcement of grafted DPNR by RC*

The RC/DPNR-graft-PS synthesis process is summarized in Figure 2. In detail, the obtained cellulose solution (4 wt.%) was slowly dropped into the DPNR-graft-PS latex under stirring condition. Then, the coprecipitation between DPNR-graft-PS and RC was performed by gradually dropping the homogenous solution into pure ethanol, followed by washing with water to eliminate the remaining of NaOH until the pH of solution became neutral. Finally, Soxhlet extraction was performed to remove the remaining homopolymer, and then the samples were dried at 50 $^{o}$C for a week to obtain the RC/DPNR-graft-PS composite. RC/DPNR-graft-PS samples were synthesized with RC and DPNR-graft-PS with ratios of 0:10, 0.5:10, 1:10, 1.5:10 and 2:10 by weight.

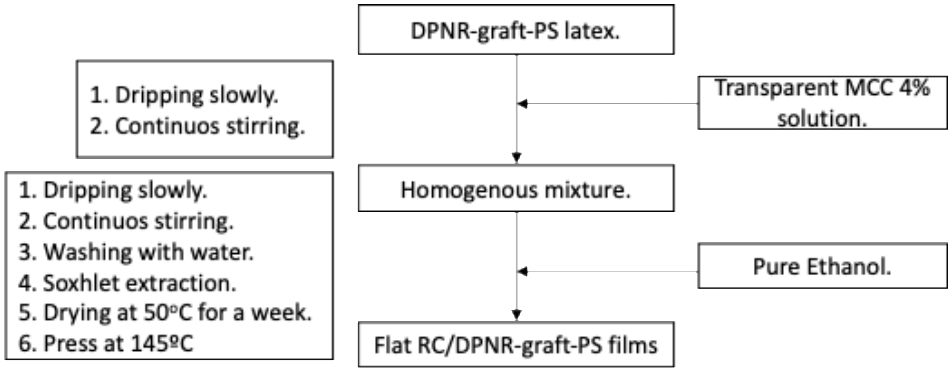


*Figure 2.* Scheme of blending RC with DPNR-graft-PS.

## 2.3. Characterizations methods

*2.3.1. Fourier transform infrared spectroscopy (FT-IR)*

Fourier transform infrared spectroscopy was used to determine the functional groups of DPNR-graft-PS and RC/DPNR-graft-PS. The infrared absorbance peaks of these samples were recorded on a Nicolet iS50 FTIR (Thermo Fisher Scientific) spectrometer in Attenuated total reflectance (ATR) mode. Samples were measured directly with a scan range from 400 $cm^{-1}$ to 4000 $cm^{-1}$. The RC/DPNR-graft-PS sample with a ratio of 1:10 was used for this measurement.

*2.3.2. X-ray diffraction (XRD)*

The crystalline parameters of samples were confirmed by X-ray diffraction measurement. XRD powder patterns were recorded on an X'Pert Pro instrument (PANalytical) under Cu kα radiation (40 kV, 35 mA). For this measurement, the RC/DPNR-graft-PS 1:10 was employed.

*2.3.3. Scanning electron microscopy (SEM)*

The morphology of the obtained samples was determined by SEM method. The RC/DPNR-graft-PS materials were pressed by a hydraulic press machine at 145 $^oC$ to obtain flat films. Cross-sectional specimens were prepared by breaking the samples in liquid nitrogen, then, the cross-sectional morphology of the samples was investigated using Hitachi TM4000Plus.

*2.3.4. Thermal gravimetric analysis (TGA)*

The thermogravimetric analysis (TGA) was used to analyze thermal properties of samples of DPNR-graft-PS and RC/DPNR-graft-PS. The measurements were made on a Linseis STA PT1600 analyzer from 25 $^oC$ to 600 $^oC$, with a heating rate of 10 $^oC$/min under a nitrogen atmosphere.

*2.3.5. Differential scanning calorimetry (DSC)*

DSC measurements were carried out to investigate the thermal characteristics of samples. Samples were packed into an aluminum pan and taken into a DSC 7020 (SII Nano Technology Inc.), the measurements were taken over a temperature range from -90 $^oC$ to 150 $^oC$ with liquid nitrogen as the coolant. The glass transition temperature ($T_g$) was determined following the ASTM E 2602 [28]. To determine $T_g$ from a heat flow curve, tangents are drawn to the baselines before and after the transition. A third tangent is drawn at the inflection point of the transition curve. The intersection points of this third tangent with the two baseline tangents are labeled $T_1$ (pre-transition) and $T_2$ (post-transition). The $T_g$ is then calculated as the average of these two temperatures: $T_g = (T_1 + T_2)/2$. This method is visually represented in Figure 3.

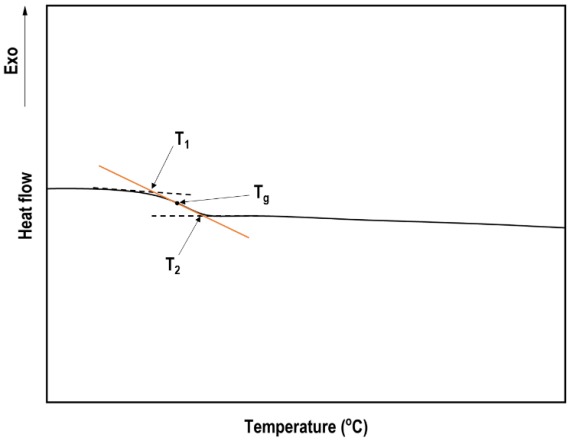


*Figure 3.* Method for determining $T_g$ via DSC.

## 3. RESULTS AND DISCUSSION

### 3.1. Characterization of RC/DPNR-graft-PS

The functional groups of DPNR-graft-PS and RC/DPNR-graft-PS were determined by FT-IR (Figure 4). The appearance of peaks at 2963, 1447, 1380, and 845 $cm^{-1}$ confirmed the characteristic structure of NR [29 - 32]. The out-of-plane bending vibration of aromatic C=C of polystyrene at 700 $cm^{-1}$ along with the decrease in the absorbance of C=C bond at 845 $cm^{-1}$ in RC/DPNR-graft-PS compared with DPNR-graft-PS owing to the breaking of C=C bond during the graft-copolymerization proves that styrene was successfully grafted onto NR [33, 34]. The appearance of the peak at 3375 $cm^{-1}$ exhibits O(3)H-O(5) hydrogen bonding of RC [35], and C-O-C pyranose ring vibration is typical for the peak at about 1036 $cm^{-1}$ [36, 37]. On the other hand, the decrease in the absorbance at 1447 $cm^{-1}$ of RC/DPNR-graft-PS compared with DPNR-graft-PS due to the formation of interpenetrating polymer network between RC and DPNR-graft-PS limits the fluctuation of the links. This, along with the new peak at 3375 $cm^{-1}$, confirms the successful incorporation of RC into the DPNR-g-PS blend.

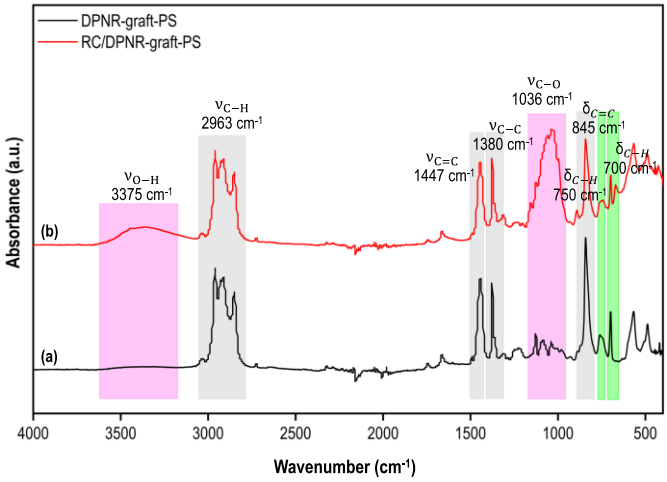


*Figure 4.* FT-IR spectrum of (a) DPNR-graft-PS and (b) RC/DPNR-graft-PS.

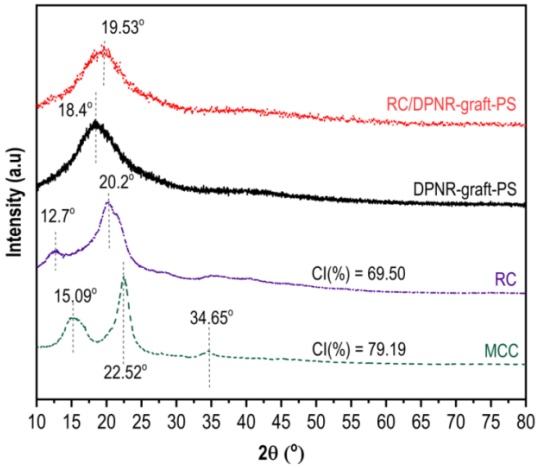


*Figure 5*. XRD of MCC, RC, DPNR-graft-PS and RC/DPNR-graft-PS.

The XRD method was utilized to determine the crystal structure of the studied samples, as illustrated in Figure 5. The result of XRD spectrum points out that RC was successfully synthesized from MCC because of the disappearance of the crystal construction of cellulose I of MCC, specifically at diffraction angles of 15.09$^o$, 22.52$^o$ and 34.65$^o$ [38]. Conversely, the presence of diffraction angle peaks at 12.7° and 20.2° is attributed to the crystal structure of cellulose II in RC [38, 39]. Besides, the formation of a new diffraction angle at 19.53$^o$ of RC/DPNR-graft-PS compared with RC and DPNR-graft-PS demonstrates that the crystal construction of cellulose II was broken during the dispersion process to form the interpenetrating polymer network indicated by the distance between the two layers of RC/DPNR-graft-PS being smaller than that of DPNR-graft-PS. Based on these findings from the XRD analysis, it can be confirmed that the synthesis of RC and RC/DPNR-graft-PS was successful.

### 3.2. Morphology of RC/DPNR-graft-PS

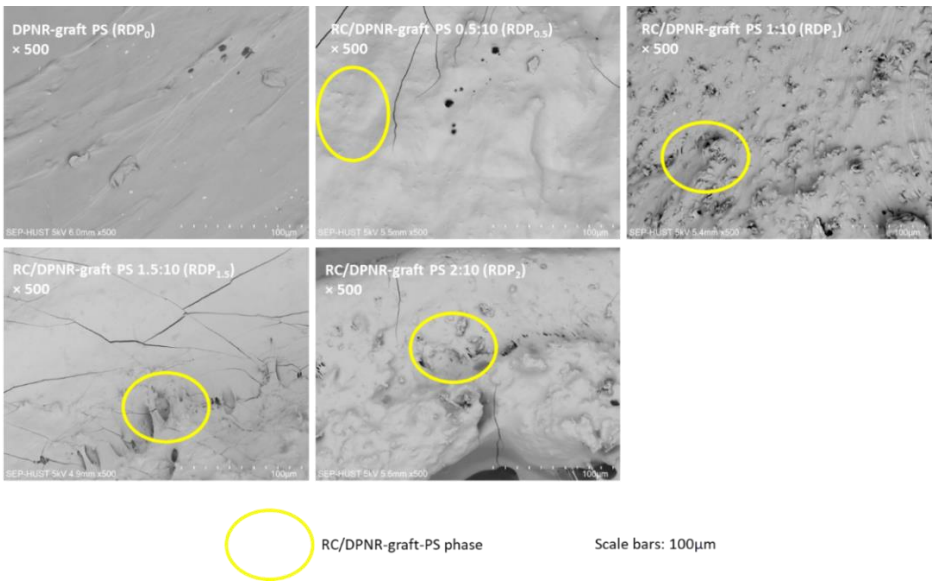


*Figure 6.* SEM images of analyzed samples with different RC : DPNR-graft-PS ratios.

The morphology of RC/DPNR-graft-PS samples was investigated by SEM (Figure 6). The SEM findings show that $RDP_0$ has a smooth and flat surface in the absence of RC. The surfaces of $RDP_{0.5}$, $RDP_1$, $RDP_{1.5}$ and $RDP_2$ become rough and uneven when RC components are introduced, among which $RDP_1$ has the most uniform surface. This is due to the fact that when the content of RC increases, RC particles tend to interact more with each other than with the DPNR-graft-PS phase, leading to the agglomeration and deposition of RC particles during the drying process. The results show that the formation of RC/DPNR-graft-PS phase of $RDP_1$ is greater than the others. Therefore, the SEM method can specify the best ratio of RC and DPNR-graft-PS (1:10).

### 3.3. Thermal properties of RC/DPNR-graft-PS

*3.3.1. Thermogravimetric analysis (TGA) and first derivative thermogravimetric analysis (DrTGA)*

The thermal properties of DPNR-graft-PS and RC/DPNR-graft-PS are presented by TGA and DrTGA in Figures 7 and 8, respectively.

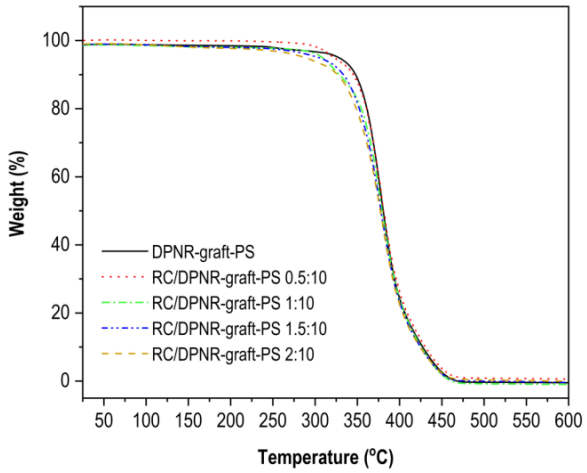


*Figure 7*. TGA of DPNR-graft-PS and RC/DPNR-graft-PS with different ratios.

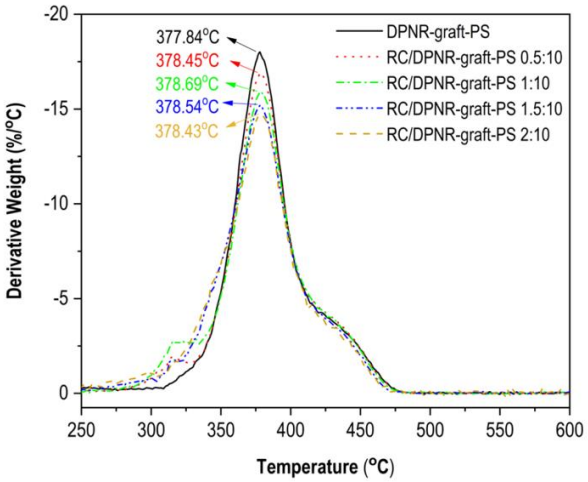


*Figure 8*. DrTGA of DPNR-graft-PS and RC/DPNR-graft-PS with different ratios.

Figure 7 shows that the decomposition of RC/DPNR-graft-PS at $T_{50\%}$ increases when increasing the RC content. It can be explained by the low thermal stability of RC leading to an increased decomposition rate of RC/DPNR-graft-PS composites [30]. Based on the DrTGA curves (Figure 8), the maximum thermal decomposition of DPNR-graft-PS is 377.84 $^{o}$C. This thermal decomposition is higher when DPNR-graft-PS is co-precipitated with RC. The maximum thermal decomposition is highest when the ratio between RC and DPNR-graft-PS is 1:10 because the interpenetrating polymer network has formed between RC and DPNR-graft-PS. When the ratio between RC and DPNR-graft-PS is 2:10, the thermal decomposition is lower than that for 1:10. It can be explained that the interpenetrating polymer network density decreases due to the agglomeration of RC particles. As a result, the composite material synthesized from RC and DPNR-graft-PS with the ratio of 1:10 gives the best thermal stability compared with other ratios. This is completely consistent with the results demonstrated above. Besides, the tendency of decomposition temperature change is also in complete agreement with the studies by Peng Yu *et al*. [40] and Visakh P. M. *et al*. [18] on the combination of RC and

NR. However, the decomposition temperatures of RC/DPNR-graft-PS samples are all higher than theirs (about 378 $^{o}$C compared to 377 $^{o}$C and 360 $^{o}$C from Peng Yu and Visakh P.M.'s studies). This verifies that the heat resistance of RC/DPNR-graft-PS is higher than RC/NR due to the presence of polystyrene segments. In addition, at a ratio of 1:10, a signal with high intensity appears at a temperature of 320 $^{o}$C, which is a characteristic signal for the decomposition temperature of cellulose (cellulose II) with DPNR-graft-PS segments. This is also in complete agreement with the study of Peng Yu [40], where the signal of RC was obtained at 320 $^{o}$C.

*3.3.2. Differential scanning thermal analysis (DSC)*

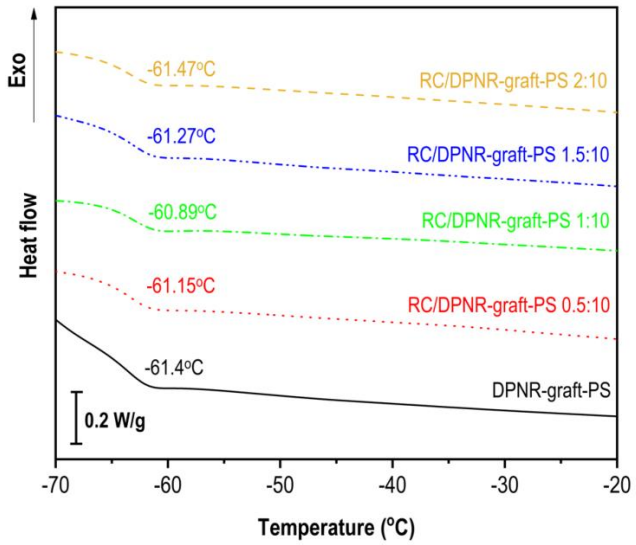


*Figure 9.* DSC curves of DPNR-graft-PS and RC/DPNR-graft-PS.

The glass transition temperature ($T_g$) of DPNR-graft-PS and RC/DPNR-graft-PS based on different RC contents were specified by DSC method (Figure 9). After co-precipitation of RC with DPNR-graft-PS, the $T_g$ of RC/DPNR-graft-PS materials increases continuously by -61.15 $^{o}$C, -60.89 $^{o}$C, -61.27 $^{o}$C, -61.47 $^{o}$C for the ratios between RC and DPNR-graft-PS of 0.5:10, 1:10, 1.5:10, 2:10, respectively, compared with -61.4 $^{o}$C of DPNR-graft-PS. The reason for this phenomena is the interference of RC segments with the mobility of DPNR-graft-PS segments owing to the formation of an interpenetration polymer network between the RC segments and the DPNR-graft-PS segments via the coprecipitation process [11]. It can be seen that the $T_g$ of RC/DPNR-graft-PS 1:10 is the highest due to the absence of agglomeration as in the case of 1.5:10 and 2:10 ratios, and this result is consistent with the results of SEM. Therefore, it can be concluded that the synthesis of RC/DPNR-graft-PS composites via the coprecipitation method is successful, and the ratio between RC and DPNR-graft-PS of 1:10 gives the best result. Comparing the $T_g$ of RC/DPNR-graft-PS in all ratios with that of NR/RC, the tendency of change in glass transition temperature is the same as in the study of Peng Yu [40]. Moreover, the $T_g$ of RC/DPNR-graft-PS samples is higher than that of NR/RC because the presence of PS increases the rotational potential energy, which leads to the restriction of motion of DPNR-graft-PS segments under the impact of heat flow. This proves that the hardness of RC/DPNR-graft-PS samples is higher than that of the NR/RC samples.

## 4. CONCLUSIONS

In conclusion, the synthesis of composites from deproteinized natural rubber by graft copolymerization with styrene and regenerated cellulose was successfully carried out. The structures of RC/DPNR-graft-PS were verified by the change in the intensity of signal peaks and the appearance of new signal peaks from FT-IR and XRD. The ascending of glass transition temperature of RC/DPNR-graft-PS when increasing the ratios between RC and DPNR-graft-PS from 0.5:10 to 2:10 in an increment of 0.5 corresponding to -61.15 $^{o}$C, -60.89 $^{o}$C, -61.27 $^{o}$C, and -61.47 $^{o}$C compared with $T_g$ of DPNR-graft-PS was attributed to the combination between RC and DPNR-graft-PS. On the other hand, based on the results of SEM and DSC, it can be concluded that the ratio between RC and DPNR-graft-PS of 1:10 is the best ratio with which the properties of the material can be improved.

***Acknowledgements.*** This research is funded by Asahi Glass Foundation (AGF.2023-01) and Ministry of Science & Technology (the Bilateral program: Joint research Vietnam-Japan), Project no. NDT/JP/23/03.

***CRediT authorship contribution statement.*** Tran Thi Tuyet: Methodology, Formal analysis. Vu Trung Nam: Methodology, Formal analysis. Nguyen Quynh Vi: Formal analysis. Nguyen Thu Ha: Investigation, Funding acquisition. Tran Thi Thuy: Investigation, Funding acquisition, Supervision. Nguyen Ngoc Mai: Investigation, Funding acquisition, Supervision.

***Declaration of competing interest.*** The authors declare that they have no known competing financial interests or personal relationships that could have appeared to influence the work reported in this paper.

## REFERENCES

1. Dieu T. V., Chuong B., Hung D. V., Tung N. H., Linh N. P. D., and Oanh D. T. Y - Review: Natural rubber - Improvement of properties, Vietnam J. Chem. **61** (2023) 269-283.
2. Trovatti, E., Carvalho, A.J., Ribeiro, S.J. and Gandini, A. – Simple green approach to reinforce natural rubber with bacterial cellulose nanofibers. Biomacromolecules **14** (2013) 2667-2674.
3. Peng Z., Kong L.X., Li S. D., Chen Y., and Huang M. F. - Self-assembled natural rubber/silica nanocomposites: Its preparation and characterization, Compos. Sci. Technol. **67** (2007) 3130-3139.
4. Chen X. and Qiu T. - Natural rubber composites reinforced with basic magnesium oxysulfate whiskers: Processing and ultraviolet resistance/flame retardant properties, Polym. Test. **81** (2020) 106271.
5. Rattanasom N., Poonsuk A., and Makmoon T. - Effect of curing system on the mechanical properties and heat aging resistance of natural rubber/tire tread reclaimed rubber blends, Polym. Test. **24** (2005) 728-732.
6. Mao Z., Wang W., and Mao G. - Improving the thermal aging resistance of γ-vulcanized polybutadiene rubber (BR)/Nature Rubber (NR) blends with sulfur added, Adv. Mater. Sci. Eng. **2021** (2021) 1-10.
7. Zhang Z., Sun J., Lai Y., Wang Y., Liu X., Shi S., and Chen X. - Effects of thermal aging on uniaxial ratcheting behavior of vulcanised natural rubber, Polym. Test. **70** (2018) 102-110.
8. Tamási K. and Kollár M. S. - Effect of Different Sulfur Content in Natural Rubber Mixture on Their Thermo-mechanical and Surface Properties, Int. J. Eng. Res. **4** (2018) 28-37.

9. Dufresne A. - Nanocellulose: a new ageless bionanomaterial, Mater. Today **16** (2013) 220-227.
10. Kumagai A., Tajima N., Iwamoto S., Morimoto T., Nagatani A., Okazaki T., and Endo T. - Properties of natural rubber reinforced with cellulose nanofibers based on fiber diameter distribution as estimated by differential centrifugal sedimentation, Int. J. Biol. Macromol. **121** (2019) 989-995.
11. Yu P., He H., Luo Y., Jia D., and Dufresne A. - Reinforcement of natural rubber: the use of in situ regenerated cellulose from alkaline–urea–aqueous system, Macromol. **50** (2017) 7211-7221.
12. Fridrihsone V., Zoldners J., Skute M., Grinfelds U., Filipova I., Sivacovs I., Spade M., and Laka M. - Dissolution of various cellulosic materials and effect of regenerated cellulose on mechanical properties of paper, Trans Tech Publ (2019) 138-144
13. Nguyen M. N., Tran T. T., Nguyen Q. T., Tran Thi T., Nguyen B. C., and Hollmann D. - Simple synthesis of cellulose hydrogels based on the direct dissolution of cellulose in tetrabutylphosphonium hydroxide followed by crosslinking, Polym. Adv. Technol. **33** (2022) 3376-3385.
14. Cai J. and Zhang L. - Rapid dissolution of cellulose in LiOH/urea and NaOH/urea aqueous solutions, Macromol. Biosci. **5** (2005) 539-548.
15. Qi H., Yang Q., Zhang L., Liebert T., and Heinze T. - The dissolution of cellulose in NaOH-based aqueous system by two-step process, Cellulose **18** (2011) 237-245.
16. Xiong B., Zhao P., Hu K., Zhang L., and Cheng G. - Dissolution of cellulose in aqueous NaOH/urea solution: role of urea, Cellulose **21** (2014) 1183-1192.
17. Zhou J. and Zhang L. - Solubility of cellulose in NaOH/urea aqueous solution, Polym. J. **32** (2000) 866-870.
18. PM, V., Thomas S., Oksman K., and Mathew A. P. - Effect of cellulose nanofibers isolated from bamboo pulp residue on vulcanized natural rubber, Bioresources **7** (2012) 2156-2168.
19. Yahya Y. R., Azura A., and Ahmad Z. - Effect of curing systems on thermal degradation behaviour of natural rubber (SMR CV 60), J. Phys. Sci. **22** (2011) 1-14.
20. Choo K., Ching Y. C., Chuah C. H., Julai S., and Liou N. S. - Preparation and characterization of polyvinyl alcohol-chitosan composite films reinforced with cellulose nanofiber, Mater. **9** (2016) 644.
21. Kim K. J. and White J. L. - Effects of regenerated cellulose and natural fiber on interfacial adhesion, rheology and crystallization property in ε-polycaprolactone compounds, Compos. Interfaces **16** (2009) 619-637.
22. Nakagaito A. N., Fujimura A., Sakai T., Hama Y., and Yano H. - Production of microfibrillated cellulose (MFC)-reinforced polylactic acid (PLA) nanocomposites from sheets obtained by a papermaking-like process, Compos. Sci. Technol. **69** (2009) 1293-1297.
23. Wang T. and Drzal L. T. - Cellulose-nanofiber-reinforced poly (lactic acid) composites prepared by a water-based approach, ACS Appl. Mater. Interfaces **4** (2012) 5079-5085.
24. Kim T., Jeon H., Jegal J., Kim J. H., Yang H., Park J., Oh D. X., and Hwang S. Y. - Trans crystallization behavior and strong reinforcement effect of cellulose nanocrystals on reinforced poly (butylene succinate) nanocomposites, RSC Adv. **8** (2018) 15389-15398.

25. Soatthiyanon N., Aumnate C., and Srikulkit K. - Rheological, tensile, and thermal properties of poly (butylene succinate) composites filled with two types of cellulose (kenaf cellulose fiber and commercial cellulose), Polym. Compos. **41** (2020) 2777-2791.
26. Dung T., Nhan N., Thuong N., Viet D., Tung N., Nghia P., Kawahara S., and Thuy T. - Dynamic mechanical properties of vietnam modified natural rubber via grafting with styrene, Int. J. Polym. Sci. **2017** (2017)
27. Dung T. A., Nhan N. T., Thuong N. T., Nghia P. T., Yamamoto Y., Kosugi K., Kawahara S., and Thuy T. T. - Modification of Vietnam natural rubber via graft copolymerization with styrene, J. Braz. Chem. Soc. **28** (2017) 669-675.
28. Moussa O., Vassilopoulos A. P., and Keller T. – Experimental DSC-based method to determine glass transition temperature during curing of structural adhesives, Constr. Build. Mater. **28** (2012) 263-268.
29. Chen D., Shao H., Yao W., and Huang B. - Fourier transform infrared spectral analysis of polyisoprene of a different microstructure, Int. J. Polym. Sci. **2013** (2013)
30. Manohar N., Jayaramudu J., Suchismita S., Rajkumar K., Reddy A. B., Sadiku E., Priti R., and Maurya D. - A unique application of the second order derivative of FTIR–ATR spectra for compositional analyses of natural rubber and polychloroprene rubber and their blends, Polym. Test. **62** (2017) 447-453.
31. Nampitch T. and Buakaew P. - The effect of curing parameters on the mechanical properties of styrene-NR elastomers containing natural rubber-graft-polystyrene, Agric. Nat. Res. **40** (2006) 7-16.
32. Ratnam C. T., Nasir M., Baharin A., and Zaman K. - Electron beam irradiation of epoxidized natural rubber: FTIR studies, Polym. Int. **49** (2000) 1693-1701.
33. Fernández-Berridi M. J., González N., Mugica A., and Bernicot C. - Pyrolysis-FTIR and TGA techniques as tools in the characterization of blends of natural rubber and SBR, Thermochimica Acta **444** (2006) 65-70.
34. Masson J. F., Pelletier L., and Collins P. - Rapid FTIR method for quantification of styrene-butadiene type copolymers in bitumen, J. Appl. Polym. Sci. **79** (2001) 1034-1041.
35. Hinterstoisser B. and Salmén L. - Application of dynamic 2D FTIR to cellulose. Vib. Spectrosc., **22** (2000) 111-118.
36. El-Sakhawy M., Kamel S., Salama A., and Tohamy H. A. S. - Preparation and infrared study of cellulose based amphiphilic materials, Journal of Cellulose Chemistry Technology **52** (2018) 193-200.
37. Pastorova I., Botto R. E., Arisz P. W., and Boon J. J. - Cellulose char structure: a combined analytical Py-GC-MS, FTIR, and NMR study, Carbohydr. Res. **262** (1994) 27-47.
38. Li M., Wei T., Qian C., and Liang Z. - Preparation of microcrystalline cellulose from Rabdosia rubescens residue and study on its membrane properties, Sci. Rep. **11** (2021) 1-9.
39. Onwukamike K. N., Tassaing T., Grelier S., Grau E., Cramail H., and Meier M. A. - Detailed understanding of the DBU/CO2 switchable solvent system for cellulose solubilization and derivatization, ACS Sustain. Chem. Eng. **6** (2018) 1496-1503.
40. Yu P., He H., and Dufresne A. - A novel interpenetrating polymer network of natural rubber/regenerated cellulose made by simple co-precipitation, Mater. Lett. **205** (2017) 202-205.